Intermetallics 53 (2014) 62–66

Contents lists available at ScienceDirect

Intermetallics

journal homepage: www.elsevier.com/locate/intermet

Effects of ion irradiation on $Zr_{52.5}Cu_{17.9}Ni_{14.6}Al_{10}Ti_5$ (BAM-11) bulk metallic glass

Alejandro G. Perez-Bergquist [a,b,*], Hongbin Bei [a], Keith J. Leonard [a], Yanwen Zhang [a,b], Steven J. Zinkle [a,b]

[a] Oak Ridge National Laboratory, Oak Ridge, TN 37831, USA
[b] University of Tennessee, Knoxville, TN 37996, USA

ARTICLE INFO

Article history:
Received 1 April 2014
Received in revised form
21 April 2014
Accepted 25 April 2014
Available online 15 May 2014

Keywords:
A. Metallic glasses
B. Irradiation effects
B. Mechanical properties
D. Microstructure

ABSTRACT

Bulk metallic glasses are intriguing candidates for nuclear applications due to their inherent amorphous structure, but their radiation response is largely unknown due to the relatively recent nature of innovations in bulk metallic glass fabrication. Here, microstructural and mechanical property evaluations have been performed on a $Zr_{52.5}Cu_{17.9}Ni_{14.6}Al_{10}Ti_5$ bulk metallic glass (BAM-11) irradiated with 3 MeV Ni^+ ions to 0.1 and 1.0 dpa at room temperature and 200 °C. Nanoindentation hardness and Young's modulus both decreased by 6–20% in samples irradiated at room temperature, with the sample irradiated to 1.0 dpa experiencing the greatest change in mechanical properties. However, no significant changes in properties were observed in the samples irradiated at 200 °C, and transmission electron microscopy showed no visible evidence of radiation damage or crystallization following ion irradiation at any of the tested conditions. These results suggest that BAM-11 bulk metallic glass may be useful for certain applications in nuclear environments.

1. Introduction

Amorphous metallic glasses were first synthesized in the 1960s [1] and have since received considerable scientific attention due to their appealing properties, including their good thermal conductivity, high strength, good ductility, and corrosion resistance [2–4]. In particular, metallic glasses are an intriguing candidate for use in radiation environments due to their lack of crystalline structure, which prohibits the formation of conventional radiation defects such as vacancy-interstitial Frenkel pairs and dislocation loops that occur in crystalline solids. Although particle irradiation can produce point defects and macroscopic changes in amorphous materials in a manner somewhat analogous to what happens in crystalline materials [5], there is some evidence that the amount of retained displacement damage can be significantly less in amorphous materials [6]. In addition, metallic glasses may possess high helium permeabilities due to their large free atomic volumes and lack of grain boundaries that can act as helium traps [6]. Finally, recent studies indicate that metallic glasses may be resistant to cavity swelling [7]. Along with the anticipated high permeability of hydrogen isotopes in metallic glasses due to their large atomic free volumes, this low cavity swelling would result in reduced tritium retention via trapping at cavities and hence would make them appealing for fusion energy applications [8].

Though metallic glasses could initially only be fabricated as thin sheets due to the extremely high cooling rates required to quench the material in the amorphous phase, pronounced advances have been made over the past few decades in metallic glass fabrication that now allow for the creation of high-performance glasses in bulk form. These new techniques have vastly increased their usefulness and created a renewed interest in these materials for structural applications [9,10]. To date, however, little data exists on the effects of displacement irradiation on these highly engineered metallic glasses. Several studies have reported crystallization of metallic glasses under ion irradiation [11–15] while others have not [7,16–20], but no systematic tests have been conducted on one specific material over a range of temperatures and ion energies (see Table 1). Similarly, electron beam irradiation studies have also largely reported crystallization of bulk metallic glasses after e-beam bombardment [21–23], though some have not [24]. Neutron irradiation studies in bulk metallic glasses are almost non-existent [25].

* Corresponding author. Oak Ridge National Laboratory, PO Box 2008 MS6138, Oak Ridge, TN 37831-6138, USA. Tel.: +1 834 576 3252.
E-mail addresses: perezbergqag@ornl.gov, alexperezbergquist@gmail.com (A.G. Perez-Bergquist).

http://dx.doi.org/10.1016/j.intermet.2014.04.016
0966-9795/

Table 1
Summary of ion irradiation studies in bulk metallic glass, organized by incident ion fluence.

Material	Ion Species	Ion energy (keV)	Ion fluence (cm^{-2})	Temp.	Crystallization (Y/N)	Source
$Zr_{50}Cu_{40}Al_{10}$	Al^+, Xe^+	5000, 200,000	1×10^{12}–3×10^{14}	RT	N	[19,20]
$Zr_{55}Cu_{30}Al_{10}Ni_5$	Ga^+	30	7×10^{14}–7×10^{15}	RT	N	[18]
$Ti_{40}Zr_{25}Be_{30}Cr_5$	C^+, Cl^+	2500	1×10^{15}–8×10^{15}	LN	N	[17]
$Zr_{61.5}Cu_{21.5}Fe_5Al_{12}$	Ar^+	300	3×10^{15}–3×10^{16}	RT	Y	[14]
$Ni_{52.5}Nb_{10}Zr_{15}Ti_{15}Pt_{7.5}$	Ni^+	1000	1×10^{16}	RT	Y	[15]
$Zr_{55}Cu_{30}Ni_5Al_{10}$	Co^+	40	7×10^{16}	140 °C	N	[16]
$Fe_{81}B_{13.5}Si_{3.5}C_2$	He^+	2800	1×10^{16}–1×10^{17}	RT	Y	[11]
$Cu_{50}Zr_{45}Ti_5$	He^+	140	1.7×10^{17}	RT	Y	[12]
$Zr_{55}Cu_{30}Al_{10}Ni_5$	Ar^+	10	2.7×10^{17}	RT	Y	[13]
$Cu_{47}Zr_{45}Al_8Y_{1.5}$	He^+	500	2×10^{17}–2×10^{18}	–	N	[7]

Though irradiation-induced softening has been reported in several studies [17,20,26,27], and hardening reported in at least one [13], mechanical properties of irradiated bulk metallic glass alloys are still largely unknown, as is the microstructural evolution of irradiated bulk metallic glasses as a function of irradiation dose and temperature. In this study, we report the results of an investigation into the effects of ion irradiation on the Zr-based metallic glass $Zr_{52.5}Cu_{17.9}Ni_{14.6}Al_{10}Ti_5$ (also known as BAM-11), a beryllium-free bulk metallic glass that exhibits excellent strength and toughness properties [28]. The microstructural evolution of the irradiated glass, studied via transmission electron microscopy, is combined with mechanical property data obtained via nanoindentation to determine the constitutive response of the irradiated material.

2. Experimental procedures

A $Zr_{52.5}Cu_{17.9}Ni_{14.6}Al_{10}Ti_5$ alloy was fabricated by arc melting in an argon atmosphere using a mixture of base metals with the following purities: 99.5% Zr, 99.99% Cu, 99.99% Ni, 99.99% Al, and 99.99% Ti. The preform alloy was then remelted and drop cast into a cylindrical copper mold of 7 mm in diameter in a Zr-gettered helium atmosphere. Sections of the drop cast rod were evaluated via X-ray diffraction (XRD) and differential scanning calorimetry, which both confirmed the material to be fully in the amorphous state. The rod was then cut into sections of 8 by 3 by 1 mm and mechanically polished to a mirror finish using progressively finer grit sand paper and finishing with a colloidal silica polish.

After fabrication, BAM-11 specimens were irradiated using 3 MeV Ni^+ ions along the surface normal. Samples were implanted to fluences of 4.2×10^{13} and 4.2×10^{14} ions/cm^2, or peak damage levels of 0.1 and 1.0 dpa, respectively, at both room temperature and elevated temperature (200 °C) at the University of Tennessee/ORNL Ion Beam Materials Laboratory (IBML, http://ibml.utk.edu/). Ion flux was measured at 2.08×10^{12} ions/cm^2 s. Ion range and damage event profiles were used to determine the fluence to dpa conversion and were generated by the SRIM software using an average displacement energy of 40 eV [29]. The ion range was calculated to be 1.36 μm, with implanted Ni concentrations reaching 5.5×10^{18} atoms/cm^3 at this depth. Damage levels at the sample surface were calculated be about 40% of peak levels. Elevated temperature irradiations were performed at 200 °C, below the known glass transition temperature of 393 °C [28].

Post-irradiation microstructural characterizations of the irradiated bulk metallic glass specimens were performed via transmission electron microscopy (TEM). TEM foils were fabricated using an FEI Quanta Dual-beam focused ion beam (FIB)/SEM with a final thinning step of 2 kV Ga^+ ions at a glancing angle of about 4° in order to minimize ion beam milling damage. Samples were then analyzed in a Phillips CM 200 TEM operating at 200 kV using the techniques of bright field (BF) imaging, selected area electron diffraction (SAED), high resolution TEM (HRTEM), and X-ray energy dispersive spectroscopy (EDS) performed in scanning TEM (STEM) mode.

Hardness and elastic modulus were measured using an MTS XP nanoindenter, with the indentations performed normal to the mechanically polished control and irradiated surfaces [30]. All tests were performed using a Berkovich diamond indenter (3 sided pyramidal tip) in continuous stiffness measurement mode at a constant indentation rate [(dP/dt)/P] of 0.05/s with a maximum applied load of 15 mN, resulting in a maximum indentation depth of ~350 nm. For statistical purposes, each sample was indented a total of ~16 times in different locations and the averages of those results are reported here. Hardness and elastic modulus were calculated using the Oliver and Pharr method [31,32]. The area function of the tip and machine stiffness of the nanoindenter were calibrated by indenting on a standard fused silica sample [33]. Because of tip bluntness, we do not report hardness and modulus data for the first 70 nm of the indentation.

3. Results and discussion

Hardness and elastic modulus data generated through nanoindentation tests are shown as a function of indenter depth in Figs. 1 and 2. Though nanoindentation measurements were taken from the sample surface up to a depth of 350 nm, only part of the data is fully indicative of the properties of material subjected to ion irradiation, as measured indentation properties are sensitive to substrate regions that are up to ten times the indenter depth [31,34]. SRIM calculations showed that peak ion deposition and peak vacancy production regions for 3 MeV Ni^+ ions in BAM-11

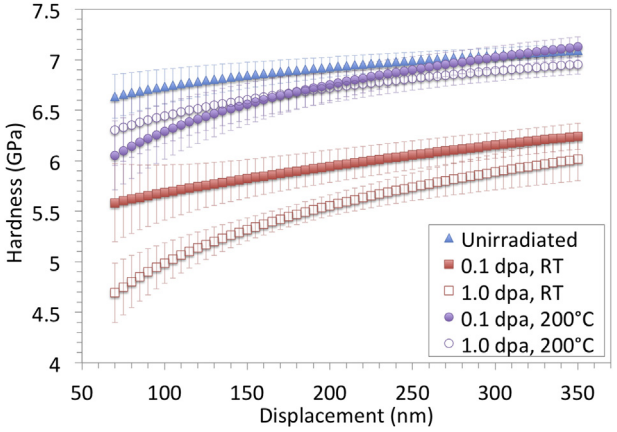

Fig. 1. Hardness as a function of indenter depth in the unirradiated and irradiated BAM-11 specimens. Error bars represent one standard deviation from the mean.

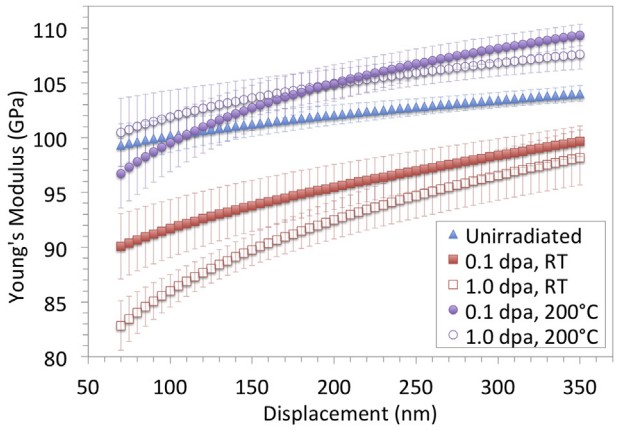

Fig. 2. Elastic modulus as a function of indenter depth in the unirradiated and irradiated BAM-11 specimens. Error bars represent one standard deviation from the mean.

Table 2
Summary of nanoindentation results on virgin and irradiated BAM-11 at a depth of 200 nm.

	Unirradiated	0.1 dpa, RT	1.0 dpa, RT	0.1 dpa, 200 °C	1.0 dpa, 200 °C
Average Hardness[a] (GPa)	6.9	5.9	5.6	6.8	6.7
Std. Dev. Of Hardness (GPa)	0.1	0.2	0.1	0.2	0.1
Average Young's Modulus[a] (GPa)	102.2	95.6	92.7	105.2	105.0
Std. Dev. Of Young's Modulus (GPa)	0.9	2.1	1.7	1.7	1.3

[a] At depth of 200 nm.

occur at a depth of around 1.5 μm, which means that mechanical behavior of samples in the near-surface region (150–200 nm indenter depth) is of the greatest interest in this study. Average data for an indenter depth of 200 nm, which represents a compromise in depth to minimize surface effects while also minimizing contributions to the data from unirradiated regions, is presented in Table 2.

Hardness and elastic modulus both decreased for the specimens irradiated at room temperature as compared to the sample in the unirradiated condition. Hardness decreased an average of about 17% from 6.9 GPa in the unirradiated state to 5.9 and 5.6 GPa in samples irradiated to 0.1 and 1.0 dpa at room temperature. Similarly, elastic modulus decreased an average of about 8% from 102.2 GPa to 95.6 and 92.7 GPa, respectively. The sample irradiated to the higher fluence level (1.0 dpa) exhibited a larger drop in both hardness and elastic modulus.

In the samples irradiated at 200 °C, the change in mechanical properties due to irradiation was much less noticeable than that due to the room temperature irradiations. Hardness in the samples irradiated at elevated temperature was relatively unchanged, with samples irradiated to 0.1 and 1.0 dpa exhibiting hardness values of 6.8 and 6.7 GPa. In addition, elastic modulus was seen to increase about 3% from 102.2 GPa in the unirradiated condition to 105.2 and 105.0 GPa in the samples irradiated to 0.1 and 1.0 dpa, respectively.

Overall, the results clearly show a significant drop in both hardness and Young's modulus in the samples irradiated at room temperature, with properties monotonically decreasing with increasing irradiation dose. The results mirror changes seen in similar ion-irradiated Zr-based bulk metallic glasses, which showed both softening and reduction in elastic modulus following irradiation to dpa levels of 0.1–10 dpa, with a more substantial drop at 100 dpa [27]. Conversely, changes in hardness in the samples irradiated at 200 °C are negligible, while changes in Young's modulus are small. It is suspected that self-healing effects, which are enhanced at high temperature, contribute to the lack of changes in mechanical properties of the BAM-11 alloy following irradiation at 200 °C.

While the mechanical properties of the ion irradiated BAM-11 alloy ranged from significant softening to negligible change depending on the specific irradiation conditions, corresponding changes in alloy microstructure were not observed. Fig. 3 shows TEM micrographs of the unirradiated alloy, including BF images at low and high magnifications, as well a diffraction pattern of the sample and a high-resolution image. Samples appeared feature-free at differing tilt conditions in the TEM, and no point defects or point defect-like structures were noticed at elevated or high resolution. Diffraction confirmed the overall amorphous nature of the specimen.

Samples irradiated to 0.1 and 1.0 dpa at both room temperature and 200 °C looked similarly feature-free and did not show any adverse microstructural effects upon radiation, as shown in Fig. 4, which displays BF TEM micrographs, DPs, and HRTEM images of each irradiated specimen. No significant changes in the microstructures of the samples were observed, selected area electron diffraction showed no change in the amorphous nature of the specimens, and high-resolution imaging did not reveal the creation of any nanocrystallites. While slight changes in the thicknesses of the diffuse halos in the electron diffraction images are visible, it is suspected that these variations arise from plural scattering effects and are a result of changes in specimen thickness, not actual differences in sample microstructure.

4. Conclusions

Amorphous BAM-11 bulk metallic glass specimens were irradiated with 3 MeV Ni^{+} ions to fluence levels of 0.1 and 1.0 dpa at

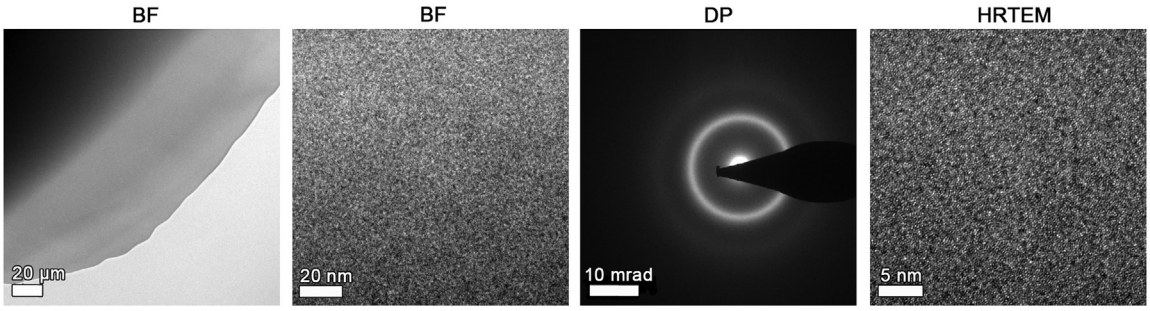

Fig. 3. BF TEM images, a diffraction pattern, and a HRTEM image of the unirradiated BAM-11 alloy.

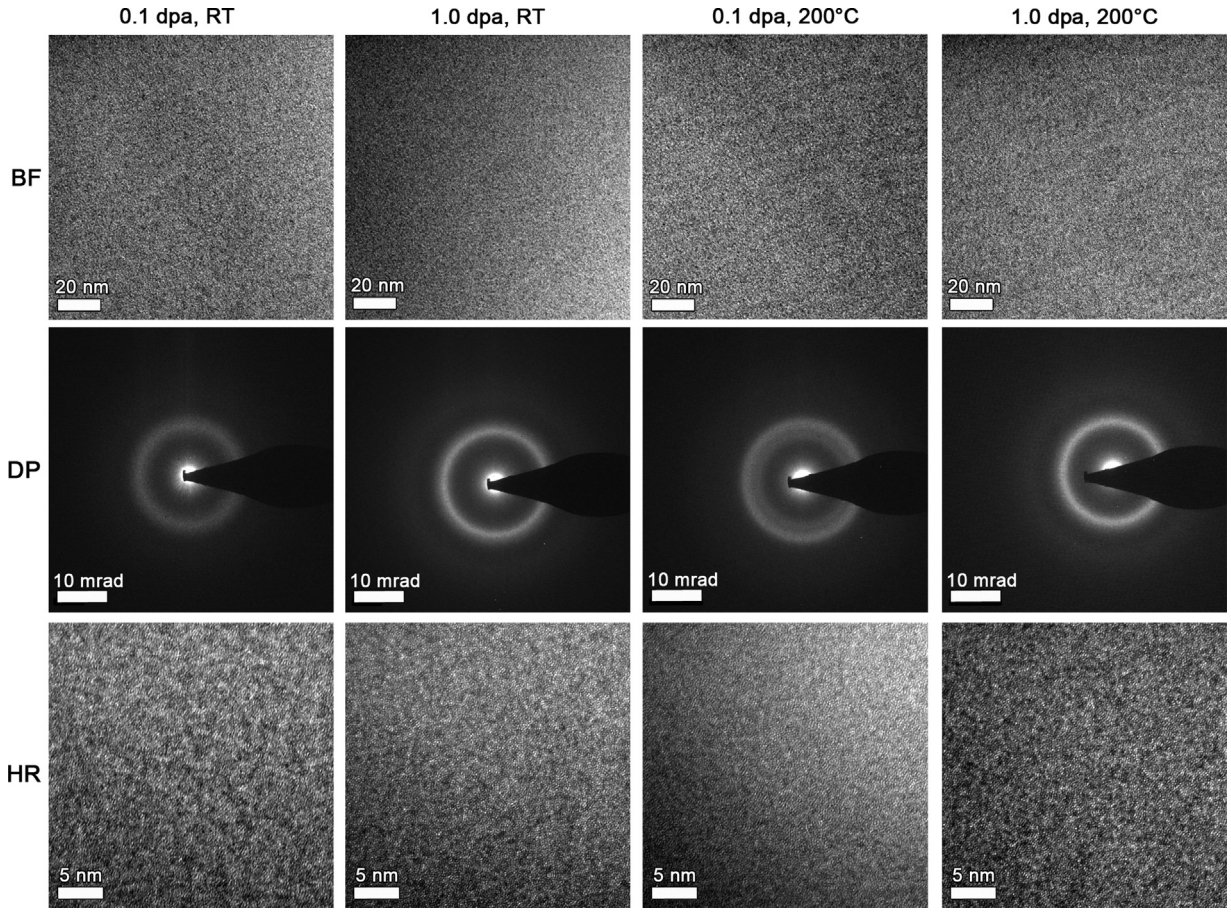

Fig. 4. TEM micrographs consisting of BF images, diffraction patterns, and high resolution images of ion-irradiated BAM-11 irradiated to 0.1 and 1.0 dpa at room temperature and 200 °C. No significant change was observed between the samples.

room temperature and 200 °C. A clear drop in hardness and elastic modulus was observed at room temperature with increasing irradiation dose, but samples irradiated at 200 °C did not experience significant changes in hardness and saw only small changes in Young's modulus. None of the tested samples exhibited any significant observable changes in microstructure.

Overall, the constitutive response of BAM-11 following irradiation to low fluence levels indicates that the alloy may have some applications as a structural material in nuclear applications where the material is utilized at elevated temperature but remains below its glassy transition temperature. However, studies of bulk metallic glasses in general seem to show a strong correlation between total dose and irradiation-induced crystallization, as shown in Table 1. For many fusion applications, bulk metallic glasses would likely undergo neutron irradiation to levels of 10–100 dpa. Therefore, further work is needed to understand the response of BAM-11 to very high fluence levels, and neutron-irradiation studies are also needed to help understand how the material would behave in a true nuclear environment.

Acknowledgments

This research was sponsored by the Office of Fusion Energy Sciences, U.S. Department of Energy under contract DE-AC05-00OR22725 with UT-Battelle, LLC. The TEM characterization utilized ORNL's Shared Research Equipment (ShaRE) User Facility, which is sponsored by the Scientific User Facilities Division, Office of Basic Energy Sciences, U.S. Department of Energy.

References

[1] Klement W, Wilens RH, Duwez P. Nature 1960;187:869.
[2] Cahn RW. Nature 1989;341:183.
[3] Chaudhari P, Turnbull D. Science 1978;199:11.
[4] Greer AL. Science 1995;267:1947.
[5] Petrusenko Y, Bakai A, Borysenko V, Astakhov A, Barankov D. Intermetallics 2009;17:246.
[6] Weber WJ, Ewing RC, Angell CA, Arnold GW, Cormack AN, Delaye JM, et al. J Mater Res 1997;12:1946.
[7] Mei X, Wang B, Dong C, Gong F, Wang Y, Wang Z. Nucl Instrum Methods Phys Res B 2013;307:11.
[8] Zinkle SJ, Snead LL. Annu Rev Mater Res 2014;44:1.
[9] Inoue A. Acta Mater 2000;44:279.
[10] Johnson WL. MRS Bull 1999;24:42.
[11] Sorescu M. J Alloys Compd 1999;284:232.
[12] Carter J, Fu EG, Bassiri G, Dvorak BM, Theodore ND, Xie G, et al. Nucl Instrum Methods Phys Res B 2009;267:1518.
[13] Iqbal M, Akhter JI, Hu ZQ, Zhang HF, Qayyum A, Sun WS. J Non Cryst Solids 2007;353:2452.
[14] Luo WD, Yang B, Chen GL. Scr Mater 2011;64:625.
[15] Myers M, Fu EG, Myers M, Wang H, Xie G, Wang X, et al. Scr Mater 2010;63:1045.
[16] Yang YZ, Tao PJ, Li GQ, Mu ZX, Ru Q, Xie ZW, et al. Intermetallics 2009;17:722.
[17] Hu Z, Zhao Z, Hu Y, Xing J, Lu T, Wei B. Mater Res 2012;15:713.
[18] Kawasegi N, Morita N, Yamada S, Takano N, Oyama T, Ashida K, et al. Appl Phys Lett 2006;89:143115.
[19] Fukumoto Y, Ishii A, Iwase A, Yokoyama Y, Hori F. J Phys Conf Ser 2010;225:012010.
[20] Onodera N, Ishii A, Fukumoto Y, Iwase A, Yokoyama Y, Hori F. Nucl Instrum Methods Phys Res B 2012;282:1.
[21] Nagase T, Umakoshi Y. Mater Trans 2005;46:608.
[22] Xie GQ, Zhang QS, Louzguine-Luzgin DV, Zhang W, Inoue A. Mater Trans 2006;47:1930.

[23] Xie GQ, Zhang QS, Louzguine DV, Zhang W, Inoue A. J Nanosci Nanotech 2007;7:3286.
[24] Sugita K, Matsumoto M, Mizuno M, Araki H, Shirai Y. J Phys Conf Ser 2008;106:012024.
[25] Nordstrom A, Rapp O, Dahlborg U. J Non Cryst Solids 1993;156–158:347.
[26] Raghavan R, Boopathy K, Ghisleni R, Pouchon MA, Ramamurty U, Michler J. Scr Mater 2010;62:462.
[27] Raghavan R, Kombaiah B, Dobeli M, Erni R, Ramamurty U, Michler J. Mater Sci Eng A 2012;532:407.
[28] Liu CT, Heatherly L, Easton DS, Carmichael CA, Schneibel JH, Chen CH, et al. Metall Mater Trans A 1998;29A:1811.
[29] Ziegler JF, Biersack JP, Littmark U. The stopping and range of ions in solids. New York: Pergamon Press; 1985. Also see: http://www.srim.org.
[30] Bei H, Lu ZP, George EP. Phys Rev Lett 2003;93:125504.
[31] Oliver WC, Pharr GM. J Mater Res 1992;7:1564.
[32] Oliver WC, Pharr GM. J Mater Res 2004;19:3.
[33] Li W, Bei H, Tong Y, Dmowski W, Gao YF. Appl Phys Lett 2013;103:171910.
[34] Samuels LE, Mulhearn TO. J Mech Phys Solids 1957;5:125.